

## Transport through multiply connected quantum wires

Sourin Das and Sumathi Rao

*Harish-Chandra Research Institute, Chhatnag Road, Jhusi, Allahabad 211019, India*

(Received 5 November 2003; revised manuscript received 19 April 2004; published 29 October 2004)

We study transport through multiply coupled carbon nanotubes (quantum wires) and compute the conductances through the two wires as a function of the two gate voltages  $g_1$  and  $g_2$  controlling the chemical potential of the electrons in the two wires. We find that there is an *equilibrium* cross-conductance, and we obtain its dependence on the temperature and length of the wires. The effective action of the model for the wires in the strong coupling (equivalently Coulomb interaction) limit can also be mapped to a system of capacitively coupled quantum dots. We thus also obtain the conductances for identical and nonidentical dots. These results can be experimentally tested.

DOI: 10.1103/PhysRevB.70.155420

PACS number(s): 71.10.Pm, 73.23.Hk, 73.63.Kv

### I. INTRODUCTION

Transport in one-dimensional systems (quantum wires) has continued to attract interest in the last decade. This has been mainly due to the fabrication of novel one-dimensional materials like single-walled carbon nanotubes, besides the more standard quantum wires obtained by gating semiconductors. Moreover, attention has been attracted by the evidence for Luttinger liquid (LL) behavior in the nonlinear transport measurements on these carbon nanotubes.<sup>1-3</sup> This has led to an upsurge of theoretical work<sup>4-6</sup> on transport through carbon nanotubes.

Transport measurements involving more than one carbon nanotube can show even more dramatic deviations from Fermi liquid behavior. For instance, the predictions<sup>7</sup> for crossed carbon nanotubes have been experimentally verified.<sup>8</sup> Further predictions<sup>9</sup> have been made for longer contacts leading to Coulomb drag as well.

In this paper, we study a system of two carbon nanotubes with a slightly different geometry. The aim is to understand the phenomena of resonant tunneling through coupled carbon nanotubes. We start with a system of two wires with density-density couplings operating at the two ends of both the wires.<sup>10</sup> This geometry is also relevant in the study of entangled electrons, where a superconductor (source of entangled electrons) is weakly coupled to the wires and the consequent nonlocal correlation is measured at the two edges.<sup>11</sup> The experimental situation that we wish to analyze is given in Fig. 1 with the schematic diagram in Fig. 2. The carbon nanotube wires are between the source and the drain and the two floating gates above the wires provide a strong capacitive coupling between the two wires at both ends. We will see later that the same setup can also be thought of as a set of two quantum dots in parallel, at least in the strong interaction limit, where the density-density couplings between the wires themselves are the tunnel barriers responsible for forming the dot. (We will see this analogy explicitly in the effective action.)

Our aim is to compute the conductance through the two wires as a function of the two gate voltages  $g_1$  and  $g_2$  controlling the density of electrons in wires 1 and 2. Without leads, when the electron-electron Coulomb interaction strength is weak, the capacitive coupling between the wires

gets renormalized to zero and the system decouples into two independent wires. The resonant transmission pattern in this case is well-known and is simply the resonant transmission between double barriers. But in the limit of strong interelectron interactions, the coupling between the wires grows, and an interesting resonance pattern emerges. With the inclusion of leads, we find that the value of the interaction strength for which the coupling changes from being irrelevant to relevant changes. With leads, even stronger inter-electron interactions are needed to access the strong coupling regime. Single-walled carbon nanotubes (SWNT), with an interaction parameter of  $K_{\text{SWNT}}=0.5-0.6$ , is essentially at the borderline between strong and weak interactions (without leads).

In Sec. II, we show how the system can be modeled in terms of the one-dimensional bosonized Luttinger liquid Lagrangian. In Sec. III, we obtain the effective action by integrating out all degrees of freedom, except at the coupling points, firstly for a uniform wire without leads. We then show that for identical wires, the system decouples in terms of symmetric (“+”) and antisymmetric (“-”) combinations of the fields at the coupling points (boundary fields), and we are essentially left with two copies of a wire with backscattering potentials at the two ends. In the weak Coulomb interaction limit, the backscattering couplings potentials renormalize to zero (at very low temperatures  $T \rightarrow 0$  and long wire lengths  $d \rightarrow \infty$ ). However, for strong Coulomb interactions, the backscattering potentials turn out to be relevant. At  $T \rightarrow 0$  and  $d \rightarrow \infty$ , the wires are “cut” and there is no transmission. However, there is still the possibility of resonant transmission. When mapped back to the original wires, the conductance

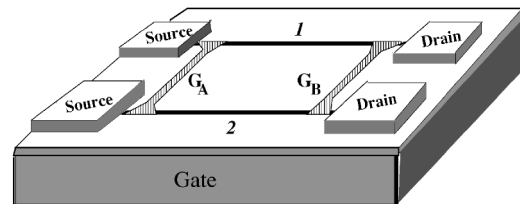


FIG. 1. Carbon nanotube wires 1 and 2 are stretched between the source and the drain.  $G_A$  and  $G_B$  are the two floating gates which generate a strong capacitive coupling between the two wires at the two ends.

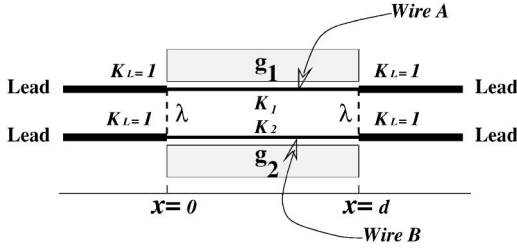


FIG. 2. Schematic diagram of the experimental setup. The wires are modeled as LLs with  $K_{i=1,2}$ , with the leads having  $K_L=1$ . The density-density coupling between the wires is denoted by its strength  $\lambda$  and the two gate voltages controlling the densities of electrons in the wire are denoted by  $g_1$  and  $g_2$ .

maxima forms an interesting resonance pattern. For nonidentical wires, there is a coupling term, which can be treated perturbatively and the change in the pattern of resonance maxima can be explicitly obtained. In both the cases of strong and weak Coulomb interactions, the conductances through the two wires can be explicitly computed in terms of the new “+” and “-” fields perturbatively. In the “high” temperature limit, the temperature  $T$  is the scale of the cutoff of the renormalization group (RG) equations and the conductances are a function of  $T$ . In the low temperature limit, and for finite length wires, the length of the wire is the RG cutoff, and the length dependences of the conductances can be obtained. Interestingly, we find that there is a nonzero *equilibrium cross-conductance*, i.e., there is a nonzero current through one wire caused by a voltage drop across the other wire. Finally, we show that the inclusion of leads changes the value of the interaction parameter where the coupling between the wires changes from being irrelevant to relevant. The resonance patterns do not change due to the inclusion of leads, but the dependence of conductances on the temperature and the length of the wires, which depend on the RG flow of the coupling strengths do change and we compute the new conductances.

In Sec. IV, we show how the effective action in the strong interaction limit is identical to the action that one would get for two capacitively coupled quantum dots. Hence, we show that our results are also applicable to a system of capacitively coupled quantum dots. Finally in Sec. V, we conclude with a discussion of how the current model can be extended to multiply coupled wires and multiply coupled dots.

## II. THE MODEL

Following Ref. 4, we will assume that the band structure of the carbon nanotube is captured by the one-dimensional free fermion model given by

$$H_0 = - \sum_{i,\alpha} \int dx v_F [\psi_{Ri\alpha}^\dagger i \partial_x \psi_{Ri\alpha} - (R \leftrightarrow L)], \quad (1)$$

where  $i=1,2$  refers to the two wires and  $\alpha=\uparrow, \downarrow$  refers to the two spins. Coulomb repulsion between the electrons can be approximated as an onsite density-density interaction as follows (Fig. 2):

$$H_{\text{int}} = \sum_i \int dx \rho_{i\uparrow} \rho_{i\downarrow}. \quad (2)$$

Here  $\rho_{i\alpha}(x) = \psi_{i\alpha}^\dagger \psi_{i\alpha}$  are the electron densities of the  $\uparrow$  and  $\downarrow$  electrons and  $\psi_{i\alpha} = \psi_{Li\alpha} e^{-ik_F x} + \psi_{Ri\alpha} e^{ik_F x}$ . The  $\psi_{Ri\alpha}$  and  $\psi_{Li\alpha}$  stand for fermion fields linearized about the left and right Fermi points in the  $i$ th wire. Using the standard bosonization procedure, whereby a fermionic theory can be rewritten as a bosonic theory with the identification  $\psi_{i\alpha} = (\eta_{i\alpha} / \sqrt{2\pi\alpha}) e^{2i\sqrt{\pi} \phi_{i\alpha}}$ , the Hamiltonian can be written as

$$H = H_0 + H_{\text{int}} = \sum_{i\beta} \frac{v_{i\beta}}{2} \left[ K_{i\beta} (\Pi_{i\beta})^2 - \frac{1}{K_{i\beta}} (\partial_x \phi_{i\beta})^2 \right], \quad (3)$$

where  $\beta=c, \sigma$  are the subscripts for charge and spin degrees of freedom, instead of  $\alpha=\uparrow, \downarrow$  since the interaction term mixes them.  $\eta_{i\alpha}$  are the Klein factors that ensure the anti-commutation relations of the fermions. Here  $K_{i\alpha} \sim (1 + g / \pi v_F)^{-1/2}$ ,  $v_{i\alpha} \sim v_F (1 + g / \pi v_F)^{1/2}$  and  $\Pi_{i,c/\sigma}$  are the fields dual to  $\phi_{i,c/\sigma}$ .  $K_{i\sigma}=1$  and  $v_{i\sigma}=v_F$  in the absence of magnetic fields.  $K_{i\alpha}=1$  for free electrons and  $K_{i\alpha}<1$  for repulsive  $e-e$  interactions.

In fact, the correct modeling of the single-wall carbon nanotube requires a four-channel LL.<sup>12</sup> Three channels are noninteracting and the fourth channel is the total charge or plasmon mode having a LL parameter ( $K_{i\alpha}$ ) which lies between 0.15 and 0.3 as estimated both from theory<sup>4,12</sup> and experiment.<sup>1</sup> The effect of all four channels can be included just by introducing the effective interaction parameter given by following replacement<sup>13</sup>

$$K_i^{-1} \rightarrow (K_i^{-1} + 3)/4 \quad (4)$$

in Eq. (3). From now on we will only work with the charge channel of the SWNT with the redefined LL parameter  $K_i$ . Hence, the action is given by

$$S = \int d\tau [L_{\text{leads}} + L_{\text{wires}} + L_{\text{coup}} + L_{\text{gates}}] \quad (5)$$

with each of the terms given below. The electrons in the leads are free while the electrons in wires 1 and 2 are interacting and they are modeled as Luttinger liquids with Luttinger parameter  $K_{iL}=1$  and  $K_i=K_1, K_2$ , respectively,

$$\begin{aligned} L_{\text{leads}} + L_{\text{wires}} &= \sum_{i=1}^2 [(L_{\text{leads}})_i + (L_{\text{wires}})_i] \\ &= \sum_{i=1}^2 \left( \int_{-\infty}^0 + \int_d^{\infty} \right) dx \mathcal{L}_i(\phi_i; K_{iL}, v_F) \\ &\quad + \sum_{i=1}^2 \int_0^d dx \mathcal{L}_i(\phi_i; K_i, v_i). \end{aligned} \quad (6)$$

Here  $\phi_i$  denotes the (spinless) Luttinger bosons in wires 1 and 2, respectively, with the Lagrangian densities

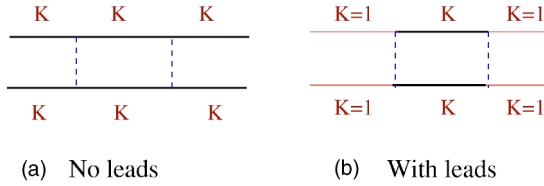


FIG. 3. Schematic diagram of the wires.

$$\mathcal{L}_i(\phi_i; K_i, v_i) = (1/2K_i)[(1/v_i)(\partial_t \phi_i)^2 - (v_i)(\partial_x \phi_i)^2]. \quad (7)$$

The Lagrangian for the coupling between the wires is given as

$$\begin{aligned} L_{\text{coup}} &= \int_{-\infty}^{+\infty} dx [\lambda_1 \rho_1(x) \rho_2(x) \delta(x) + \lambda_2 \rho_1(x) \rho_2(x) \delta(x-d)] \\ &= \frac{\lambda}{(\pi\alpha)^2} [\cos(2\sqrt{\pi}\phi_1^1) \cdot \cos(2\sqrt{\pi}\phi_2^1) + \cos(2\sqrt{\pi}\phi_1^2) \\ &\quad + 2k_F d] \cdot \cos(2\sqrt{\pi}\phi_2^2 + 2k_F d), \end{aligned} \quad (8)$$

where  $\rho_i$  are the densities of the electrons, and in terms of the bosonic fields, they are given by

$$\rho_i(x) = \frac{1}{\sqrt{\pi}} \partial_x \phi_i(x) + \frac{1}{\pi\alpha} \cos(2\sqrt{\pi}\phi_i(x) + 2k_F x). \quad (9)$$

Here  $\alpha$  is an infrared regulator and we have set Klein factors to 1 (which is sufficient for the correlation functions we compute in this paper, although in general with two wires, one has to be careful). The gate voltage that couples to the electrons densities in the two dots is modeled by the following term in the action:

$$L_{\text{gates}} = \sum_{i=1}^2 g_i \int_0^d dx \rho_i(x) = \sum_{i=1}^2 \frac{g_i}{\sqrt{\pi}} (\phi_i^2 - \phi_i^1). \quad (10)$$

### III. THE EFFECTIVE ACTION

We first analyze the model of a uniform quantum wire with

$$S = \int d\tau (L_{\text{wires}} + L_{\text{coup}} + L_{\text{gates}}), \quad (11)$$

where  $L_{\text{wires}} = \sum_{i=1}^2 \int_{-\infty}^{\infty} \mathcal{L}_i(\phi_i; K_i, v_i)$ . The wire both to the left of the first coupling point and the right of the second coupling point are interacting wires with the same interaction parameter as the wire between the two coupling points, as shown in Fig. 3(a). Such a model would be relevant for two extremely long carbon nanotubes coupled together at two points, near the middle. The terms in the Lagrangian for the coupling between the wires  $L_{\text{coup}}$  and the coupling between the wires and the gates,  $L_{\text{gates}}$ , are both functionals only of the fields at the boundaries (i.e., at  $x=0$  and  $x=d$ ). Hence, even in  $L_{\text{wires}}$  (which is a functional of the bulk fields), it is convenient for further calculations to integrate out all degrees of freedom except at the coupling points,  $x=0$  and  $x=d$ , and

obtain an effective action<sup>14</sup> in terms of the boundary fields given by

$$\begin{aligned} (S_{\text{eff}})_0 &= \int d\tau \sum_{i=1}^2 (L_{\text{wires}})_i = \sum_{i=1}^2 \frac{1}{2K_i} \int |\omega| ((\tilde{\phi}_i^1)^2 + (\tilde{\phi}_i^2)^2) d\omega \\ &\quad + \sum_{i=1}^2 \frac{1}{2K_i} \int \frac{|\omega|}{e^{k_i d} - e^{-k_i d}} \{ (e^{k_i d} + e^{-k_i d}) ((\tilde{\phi}_i^1)^2 + (\tilde{\phi}_i^2)^2) \\ &\quad - 4\tilde{\phi}_i^1 \tilde{\phi}_i^2 \} d\omega. \end{aligned} \quad (12)$$

The Fourier transformed tilde fields are defined by  $\phi_i^{1,2}(\tau) = \sum_{\omega_n} e^{-i\omega_n \tau} \tilde{\phi}_i^{1,2}(\omega_n)$ . In the high frequency or equivalently, high temperature limit, ( $T \gg \hbar v_i / k_B d$ ),  $(S_{\text{eff}})_0$  reduces to

$$(S_{\text{eff}})_0^{\text{ht}} = \sum_{i=1}^2 \frac{1}{K_i} \int |\omega| ((\tilde{\phi}_i^1)^2 + (\tilde{\phi}_i^2)^2) d\omega. \quad (13)$$

Let us now also include the contributions coming from the long range part of the Coulomb interaction explicitly (by hand),<sup>15</sup> since conventional LL theory does not automatically include these contributions. They are incorporated by including the term

$$\int d\tau \sum_{i=1}^2 \frac{Q_i^2}{2C_i} = \frac{U_{Ci}}{2} \int d\tau \sum_{i=1}^2 (\phi_i^2 - \phi_i^1)^2 \quad (14)$$

in the effective action. Here the  $Q_i$  stands for the excess accumulated charge with respect to the background in the confined region of double barrier and  $C_i$  is the corresponding capacitance. With this, in the low temperature limit ( $T \ll \hbar v_i / k_B d$ ), the density-density coupling at the two ends of each wire are seen coherently by the electrons and the total effective action reduces to

$$\begin{aligned} S_{\text{eff}} &= (S_{\text{eff}})_0^{\text{ht}} + \int d\tau [L_{\text{coup}} + L_{\text{gates}}] \\ &= \sum_{i=1}^2 \frac{1}{2K_i} \int |\omega| ((\tilde{\phi}_i^1)^2 + (\tilde{\phi}_i^2)^2) d\omega \\ &\quad + \int d\tau \left[ \sum_{i=1}^2 \frac{U_i}{2} (\phi_i^2 - \phi_i^1)^2 + L_{\text{coup}} + L_{\text{gates}} \right]. \end{aligned} \quad (15)$$

Here  $U_i = \hbar v_i / K_i d + U_{Ci} = \Delta_i / K_i + U_{Ci}$  are the mass terms that suppress charge fluctuations on the wires and are responsible for the Coulomb blockade (CB) through the wires.  $\Delta_i$  is the discrete level spacing of the plasmon state in the double barrier system. In this paper, we ignore the extra effects that occur due to the discreteness of these levels. These have been discussed in Refs. 16–18. Note that for weak interactions, where  $K_i \sim 1$  and  $U_{Ci}$  is very small,  $U_i \sim \Delta_i$  the Coulomb blockade levels are the same as the plasmon levels.

In this paper we consider the case where the coupling between the wires are symmetric,  $\lambda_1 = \lambda_2 = \lambda$  (say). For further analysis, it is convenient to define the following variables:

$$\theta_i = \frac{\phi_i^1 + \phi_i^2}{2} + \frac{k_F d}{2}, \quad N_i = \frac{\phi_i^2 - \phi_i^1}{\sqrt{\pi}} + \frac{k_F d}{\pi}. \quad (16)$$

In terms of these variables the coupling part of the action can be written as

$$L_{\text{coup}} = \frac{\lambda}{\pi\alpha} [\cos 2\sqrt{\pi}(\theta_1 + \theta_2) \cos 2\sqrt{\pi}(N_1 + N_2) + \cos 2\sqrt{\pi}(\theta_1 - \theta_2) \cos 2\sqrt{\pi}(N_1 - N_2)]. \quad (17)$$

The expression for  $L_{\text{coup}}$  in terms of the new fields suggests that we can diagonalize the problem by introducing the following symmetric and antisymmetric combination of fields:

$$\theta_{\pm} = \theta_1 \pm \theta_2, \quad N_{\pm} = N_1 \pm N_2. \quad (18)$$

Thus, the total action (in the low  $T$  limit) can be written in terms of these new  $\pm$  fields as

$$S_{\text{eff}} = \int d\tau \left[ \sum_{\nu=+,-} \left[ \frac{\mathcal{U}_{\text{eff}}}{2} (N_{\nu} - N_{0\nu})^2 \right] + \frac{\mathcal{U}_1 - \mathcal{U}_2}{4} N_+ N_- + \frac{\lambda}{(\pi\alpha)^2} \sum_{\nu=\pm} [\cos 2\sqrt{\pi}\theta_{\nu} \cos \pi N_{\nu}] \right], \quad (19)$$

where  $\mathcal{U}_{\text{eff}} = (\mathcal{U}_1 + \mathcal{U}_2)/4$ ,  $\mathcal{U}_i = \pi U_i$  and  $S_i$ ,  $N_{0+}$ , and  $N_{0-}$  are given by

$$S_i = \frac{1}{2} \sum_{\omega_n} \left[ (\tilde{N}_+)^2 + \frac{\pi}{4} (\tilde{\theta}_+)^2 + (\tilde{N}_-)^2 + \frac{\pi}{4} (\tilde{\theta}_-)^2 \right] \quad (20)$$

and

$$N_{0\pm} = \frac{k_F d (\mathcal{U}_1 \pm \mathcal{U}_2) - (g_1 \pm g_2)}{(\pi/2)(\mathcal{U}_1 + \mathcal{U}_2)}. \quad (21)$$

Thus, from Eq. (19), we see that when  $\mathcal{U}_1 = \mathcal{U}_2$ , we have successfully mapped the problem of two density coupled quantum wires to a pair of “decoupled” quantum wires with double barriers. When  $\mathcal{U}_1 \neq \mathcal{U}_2$  but is *small*, the two wires interact weakly. It is also possible to identify effective Luttinger liquid parameters for the “ $\pm$ ” wires from  $\mathcal{U}_{\text{eff}}$  (for  $\mathcal{U}_1 = \mathcal{U}_2$ ) by writing it as  $\mathcal{U}_{\text{eff}} = \pi U_{\text{eff}} = \pi \hbar v / K_{\text{eff}} d$  and we find that  $K_{\text{eff}} = 4K_1 K_2 / (K_1 + K_2)$  for both the “+” and “-” wires, since both of them have the same  $\mathcal{U}_{\text{eff}}$ .

Note that for  $K_1 = K_2 = K$ ,  $K_{\text{eff}} = 2K$ . Hence, the interaction parameter has doubled<sup>7</sup>. The “+” and “-” wires are “free” when  $K = 1/2$ , and the quasiparticles have repulsive interactions for  $K < 1/2$  and attractive interactions for  $K > 1/2$ .

#### A. Case of $\mathcal{U}_1 = \mathcal{U}_2 = \mathcal{U}$

When  $\mathcal{U}_1 = \mathcal{U}_2$ , the coupling term between the “+” and “-” fields drops from the effective action and the action is exactly identical to the effective action of a decoupled pair of quantum wires, each with two barriers, in one dimension.<sup>14</sup> The action remains invariant under the following transformations

$$\theta_{\pm} \rightarrow \theta_{\pm} + \frac{\sqrt{\pi}}{2}, \quad N_{\pm} \rightarrow 2N_{0\pm} - N_{\pm}, \quad (22)$$

when  $N_{0\pm}$  is tuned to be a half-integer by tuning the gate voltages  $g_1$  and  $g_2$ . This tuning of gate voltages corresponds to certain special points in the  $(g_1, g_2)$  plane where resonance transport of electrons through each of the wires takes place.

The conductance matrix for the two-wire system in the linear response regime, can be written as

$$G = \begin{pmatrix} G_{11} & G_{12} \\ G_{21} & G_{22} \end{pmatrix}, \quad (23)$$

where  $G_{ii}$  is the conductance through each wire due to the voltage across the same wire and  $G_{ij}$  is the cross-conductance—the conductance in wire  $i$  due to the voltage drop in wire  $j$ . Note that the density-density couplings at the two ends of the wires can be thought to be the source of “entanglement” of the previously uncorrelated electrons in wires 1 and 2. The cross-conductance  $G_{12}$  is a measure of this entanglement.

By transforming to the “+” and “-” wires, we can compute  $G_{\pm}$  explicitly since they are just the conductances for uncoupled wires with two barriers each. Moreover, since  $G_{\pm}$  can be written in terms of the currents  $j_{\pm} = j_1 \pm j_2$ , we find that

$$G_+(g_1 + g_2) = (G_{11} + G_{22} + G_{12} + G_{21})(g_1, g_2),$$

$$G_-(g_1 - g_2) = (G_{11} + G_{22} - G_{12} - G_{21})(g_1, g_2), \quad (24)$$

from which we can obtain

$$G_1 + G_2 = G_+ + G_- = G, \quad (25)$$

$$G_{12} + G_{21} = G_+ - G_-. \quad (26)$$

Note that  $G_{12} + G_{21} \neq 0$ , as long as  $G_+ \neq G_-$ . Thus unlike in the case of the singly crossed carbon nanotubes,<sup>7</sup> where the cross-conductance  $G_{12}$  was a nonequilibrium effect and vanished in the linear response regime, here, *the cross-*

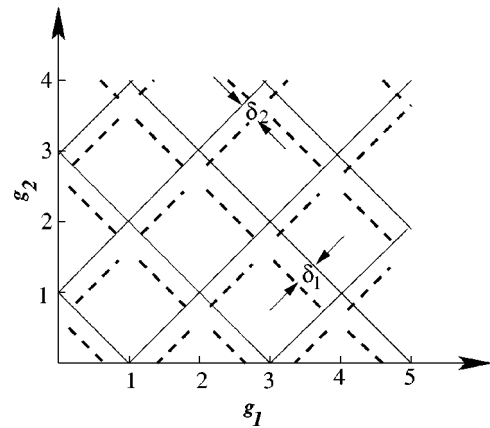


FIG. 4. Conductances in the plane of the two gate voltages  $g_i$ . For  $\mathcal{U}_1 = \mathcal{U}_2$ , the solid lines represent semi-maxima (“+” or “-” wire at resonance) and the crossings represent the maxima (both wires at resonance). The dotted line represents semimaxima (“+” or “-” wire at resonance) for  $\mathcal{U}_1 \neq \mathcal{U}_2$ . There is no resonance at the crossings of the dotted lines and that region has been left blank.

conductance is an equilibrium phenomena. It only requires  $G_+ \neq G_-$ . Since the conductances  $G_+$  and  $G_-$  are independently tuned by the gate voltages  $g_1 + g_2$  and  $g_1 - g_2$ , they are equal only if they are both tuned to be equal.

The combined transport through the wires 1 and 2 can now be tuned to resonance when both  $G_+$  and  $G_-$  are tuned to resonance (maximum), or when one of them is tuned to resonance (semimaximum). It is easy to see that the conductance maxima through both the dots form a rectangular grid of points in the plane of the gate voltages, when  $N_{0+}$  and  $N_{0-}$  are tuned to half integers, i.e.,  $N_{0+} = n + 1/2$  and  $N_{0-} = m + 1/2$ . The values of the appropriate gate voltages, given below,

$$g_2 + g_1 = \left[ \frac{2k_F d}{\pi} - \left( n + \frac{1}{2} \right) \right] \mathcal{U},$$

$$g_2 - g_1 = \left[ \left( m + \frac{1}{2} \right) \right] \mathcal{U}, \quad (27)$$

are plotted in Fig. 4. The semimaxima form the two pairs of solid lines and the intersections of the two pairs of lines are the maxima.

### 1. Weak interaction, weak coupling limit

After transforming to the “ $\pm$ ” wires, the RG flow of the density-density coupling term is given by

$$\frac{d\lambda}{dl} = (1 - K_{\text{eff}})\lambda. \quad (28)$$

For weak interelectron interactions ( $K > 1/2$  or  $K_{\text{eff}} > 1$ ), the  $\lambda$  coupling is irrelevant and it grows smaller as a function of the energy cutoff  $l = F \ln[\Lambda(\lambda)/\Lambda]$ . Here,  $\Lambda$  is an arbitrary high energy scale (say, the inverse of the average interparticle separation) at which we start the renormalization group flow. We are interested in the conductance of the system in the low temperature limit ( $T \ll T_d$ ) where there is coherent transport through both the barriers. The total conductance through the system is given by<sup>15</sup>

$$G = \frac{2e^2}{h} - \frac{\alpha}{2} e^2 \lambda^2 \left( \frac{T}{\Lambda} \right)^{2(K_{\text{eff}}-1)} \times [2 + \cos 2\pi N_{0+} + \cos 2\pi N_{0-}], \quad (29)$$

where  $\alpha$  is an arbitrary constant of order unity. Note that the last factor (i.e., factor in square bracket) goes to zero when both the wires are tuned to resonance and then there is perfect conductance through both the wires.

Similarly, the temperature dependence of the total cross-conductance is given by

$$G_{12} + G_{21} = \frac{\alpha}{2} e^2 \lambda^2 \left( \frac{T}{\Lambda} \right)^{2(K_{\text{eff}}-1)} (\cos 2\pi N_{0+} - \cos 2\pi N_{0-}) \quad (30)$$

in the low temperature limit. Thus, the cross-conductance is nonzero unless both wires are at resonance or  $N_{0+} = N_{0-} + 2\pi N$  and it can be both negative or positive depending on the gate voltages ( $g_1, g_2$ ) operating on the two wires. Note

also that as the temperature is reduced, the effective barrier strength reduces and hence, perturbation theory is a good approximation. In fact, for  $T \rightarrow 0$ , the direct conductances are very close to  $e^2/h$  or perfect conductance and the cross-conductances go to zero.

### 2. Strong interaction, strong coupling limit

For strong interelectron interactions ( $K_{\text{eff}} < 1$ ) or  $K < 1/2$ , the density-density coupling term is relevant under the RG transformation. At low energies, the strength of the barriers  $\lambda$  renormalize to very large values, and in fact, at zero temperature, or for very long wires, the “+” and “-” wires are cut and there is no transmission, except at resonance points (which are the points where the Coulomb blockade is lifted). Note also that the discreteness of the plasmon levels, in general, implies that for small dots, the Coulomb blockade peaks get paired, because each level can accommodate both  $\uparrow$  and  $\downarrow$  spins. So the CB level spacing alternates between  $U_C$  and  $U_C + \Delta_i/K$ . For large dots, this difference is negligible. But for small dots, this difference is experimentally significant and is the basis of the observation of the Kondo effect in small dots.<sup>21</sup> Zero transmission away from resonance points is true only at  $T=0$  and for infinite length wires. For finite temperatures and for finite length wires, there are power law conductances even when Coulomb blockade is not lifted, given by<sup>14</sup>

$$G \sim e^2 t^2 \left( \frac{T}{\Lambda} \right)^{2(1/K_{\text{eff}}-1)} \sim G_{12} + G_{21}, \quad (31)$$

where  $t$ , of order  $1/\lambda$ , is a tunneling amplitude between the cut wires. In this limit, the system can be considered as a pair of decoupled dots, (“+” and “-” dots) which are tunnel-coupled to Luttinger wires [see Fig. 7(b) below]. The density-density couplings which grow themselves act as the barriers forming the dot.

Let us now incorporate the leads, by studying the model in Eq. (5). The leads have noninteracting electrons and only the electrons within the length of the wire between the two coupling terms are interacting [see Fig. 3(b)].

The inclusion of leads essentially changes the renormalization group flow of the barriers in the two wires.<sup>15,19,20</sup> To find the new RG flows, we first note that even with the inclusion of leads, it is convenient to work with the “+” and “-” fields, where the two wires decouple. In terms of these fields, we find that the interaction parameters in the leads are also changed and are given by  $K_{\pm L} = 2$  as compared to  $K_i = 1$ . Hence, the leads are no longer “free” in the new basis. (Note that the real leads are of course free. We have mapped the model to another model in terms of the  $\pm$  fields, where the “effective” leads just appear interacting.)

When the barrier is at the boundary between the leads and the wire as in our set-up in Figs. 1 and 2, the RG equations are given by<sup>20</sup>

$$\frac{d\lambda}{dl} = \begin{cases} (1 - K'_{\text{eff}})\lambda & T \gg T_d \\ (1 - K_{\pm L})\lambda & T \ll T_d \end{cases}$$

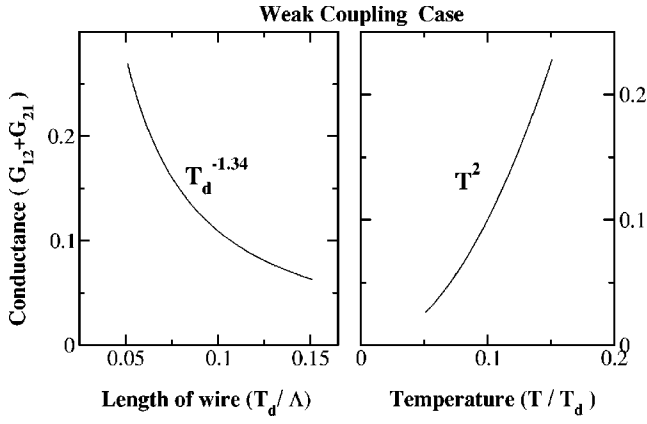


FIG. 5. The dependence of the low temperature ( $T \ll T_d$ ) cross-conductance (in units of  $2e^2/h$ ) on  $T$  and  $T_d$  for the case of  $K = 0.5$ . Here  $T_d = \hbar v/k_B d$  is the temperature equivalent of the length  $d$  of the wire.  $\Lambda$  is the high energy cutoff scale. The overall scale of the conductance has been adjusted by adjusting  $\alpha$ , to be within the perturbative regime. Hence, it is only the power law which is significant.

where  $K'_{\text{eff}} = 2 K_{\text{eff}} K_{\pm L} / (K_{\text{eff}} + K_{\pm L}) = 4K / (K + 1)$  and  $T_d = \hbar v/k_B d$  as before. So for the “ $\pm$ ” wires,  $\lambda$  is relevant if  $K'_{\text{eff}} < 1$ , i.e.,  $K < 1/3$  and it is relevant for  $K'_{\text{eff}} > 1$ , i.e.,  $K > 1/3$ .

For “weak” interelectron interactions ( $K'_{\text{eff}} > 1$ ) or  $K > 1/3$ , the density-density coupling term is irrelevant under the RG transformation. Note that connecting leads to the interacting wires, changes the values of  $K$  for which the density-density coupling is irrelevant from  $K \geq 1/2$  to  $K \geq 1/3$ . So we observe that even if  $K < 1/2$ , but  $K > 1/3$ , the density-density coupling still remains irrelevant, unlike the case of uniform wire with no leads.

The high temperature conductance scales now with  $K'_{\text{eff}}$  instead of  $K_{\text{eff}}$ . But at low temperatures ( $T \ll T_d$ ) where there is coherent transport through both the barriers, there exists a new feature. The conductance now has both non-trivial temperature and length dependences and is given by

$$G = \frac{2e^2}{h} - \frac{\alpha}{2} e^2 \lambda^2 \left( \frac{T}{T_d} \right)^{2(K_{\pm L} - 1)} \left( \frac{T_d}{\Lambda} \right)^{2(K'_{\text{eff}} - 1)} \times (2 + \cos 2\pi N_{0+} + \cos 2\pi N_{0-}). \quad (32)$$

The temperature dependence essentially comes because in the “ $\pm$ ” wires, the leads are no longer free.

Similarly, the temperature and length dependences of the total cross-conductance is given by

$$G_{12} + G_{21} = \frac{\alpha}{2} e^2 \lambda^2 \left( \frac{T}{T_d} \right)^{2(K_{\pm L} - 1)} \left( \frac{T_d}{\Lambda} \right)^{2(K'_{\text{eff}} - 1)} \times (\cos 2\pi N_{0+} - \cos 2\pi N_{0-}). \quad (33)$$

This result is experimentally testable and is plotted in Fig. 5.

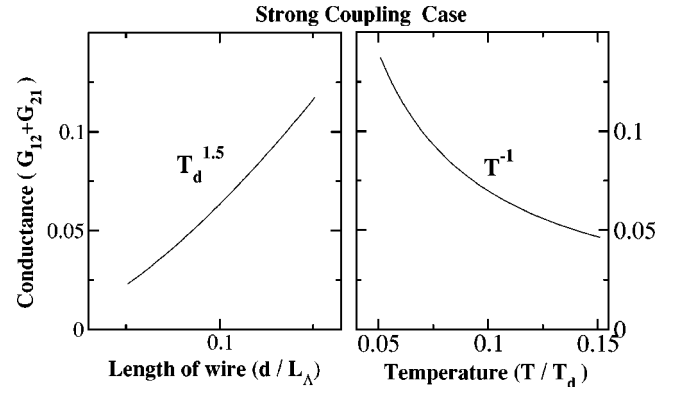


FIG. 6. The dependencies of the low temperature ( $T \ll T_d$ ) conductance (in units of  $2e^2/h$ ) on  $T$  and  $T_d$  for the case of  $K = 0.25$ .

For strong interelectron interactions ( $K'_{\text{eff}} < 1$ ) or  $K < 1/3$ , the density-density coupling term is relevant under the RG transformation. Connecting leads to the interacting wires changes the regime of  $K$  for which the density-density coupling is relevant from  $K < 1/2$  to  $K < 1/3$ . Since  $\lambda$  renormalizes to very large values in this regime, for very long wires or at very low temperature, the “+” and “-” wires are cut and there is no transmission, except at resonance points. However, for finite temperatures and for finite length wires, as usual, we can compute the conductances as a function of the temperature and/or length scale perturbatively. The high temperature ( $T \gg T_d$ ) conductance scales now with  $1/K'_{\text{eff}}$ , instead of  $K'_{\text{eff}}$  as in the weak interaction case. At low temperatures ( $T \ll T_d$ ) also, the interaction parameters get replaced by their inverses<sup>14,20</sup> and the direct and cross-conductances are given by

$$G \sim e^2 t^2 \left( \frac{T}{T_d} \right)^{2(1/K_{\pm L} - 1)} \left( \frac{T_d}{\Lambda} \right)^{2(1/K'_{\text{eff}} - 1)} \sim G_{12} + G_{21}, \quad (34)$$

where  $t$  is the tunneling between the cut wires. This result is also experimentally testable and is plotted in Fig. 6.

## B. Case of $\mathcal{U}_1 \neq \mathcal{U}_2$

However, when  $\mathcal{U}_1 \neq \mathcal{U}_2$ , it is no longer possible to tune for resonances through the “+” and “-” wires simultaneously due to the presence of the  $N_+ N_-$  term in the effective action.  $N_{0+}$  now depends on  $N_-$  and  $N_{0-}$  depends on  $N_+$ . But it is always possible to fix either  $N_{0-}$  or  $N_{0+}$  and tune the other wire to resonance. The condition for resonance for the  $\pm$  wire is given by

$$V_{\text{eff}}(N_{\pm}, \theta_{\pm}; N_{\mp}, \theta_{\mp}) = V_{\text{eff}} \left( N_{\pm} + 1, \theta_{\pm} + \frac{\sqrt{\pi}}{2}; N_{\mp}, \theta_{\mp} \right) \quad (35)$$

and the appropriate gate voltages at which the wires get tuned to resonance is given by

$$g_1 + g_2 = \left[ \frac{2k_F d}{\pi} - \left( n + \frac{1}{2} \right) - \frac{\pi}{4} \left( \frac{\mathcal{U}_1 - \mathcal{U}_2}{\mathcal{U}_1 + \mathcal{U}_2} \right) \right] \mathcal{U}_{\text{eff}},$$

$$g_1 - g_2 = \left[ \frac{2k_F d}{\pi} \left( \frac{\mathcal{U}_1 - \mathcal{U}_2}{\mathcal{U}_1 + \mathcal{U}_2} \right) - \left( m + \frac{1}{2} \right) - \frac{\pi}{4} \left( \frac{\mathcal{U}_1 - \mathcal{U}_2}{\mathcal{U}_1 + \mathcal{U}_2} \right) \right] \mathcal{U}_{\text{eff}},$$
(36)

which gives us the deviations  $\delta_1$  and  $\delta_2$  in Fig. 4 as

$$\delta_1 = \frac{\pi}{4} \left( \frac{\mathcal{U}_1 - \mathcal{U}_2}{\mathcal{U}_1 + \mathcal{U}_2} \right) \mathcal{U}_{\text{eff}},$$
(37)

$$\delta_2 = \left( \frac{k_F d}{2\pi^2} - 1 \right) \delta_1.$$
(38)

Here  $n$  and  $m$  are the number of electrons on the  $+/-$  wires when they are off resonance and the  $-/+$  wire is tuned to resonance. Since the resonance condition of one wire (say wire A) depends on the number of electrons of the other wire (wire B), unlike the case when the two wires are decoupled ( $\mathcal{U}_1 = \mathcal{U}_2$ ), wire B clearly has to have a fixed number of electrons, i.e., it has to be off-resonance. (At resonance, the wire is degenerate for  $n$  and  $n+1$  electrons and hence does not have a fixed number of electrons. The electron number fluctuates.) So the derivations of the gate voltages above for the  $+/-$  wires are valid only when the  $-/+$  wire is far from resonance. Our analysis is unable to predict conductances for  $\mathcal{U}_1 \neq \mathcal{U}_2$  when both the wires are near resonance.

#### IV. EFFECTIVE ACTION OF COUPLED DOTS

In this section, we map the effective action studied in the earlier section to the effective action of capacitively coupled quantum dots to obtain the conductance pattern for coupled dot systems.

We note that Eq. (19) is precisely the effective action of coupled quantum dots with charging energies  $\mathcal{U}_{\text{eff}}$  and an interaction energy  $(\mathcal{U}_1 - \mathcal{U}_2)/4$ . In the absence of the interaction term, i.e., when  $\mathcal{U}_1 = \mathcal{U}_2$ , by tuning  $N_{0\nu}$ , or equivalently by tuning  $g_i$  the dot states with  $N_\nu$  and  $N_\nu + 1$  can be made degenerate. This is the lifting of the Coulomb blockade (CB) for each individual dot. The gate voltages at which both the CB's are lifted and the current through both dots is at a maximum are the same points in Fig. 4 where both the wires go through a resonance. Similarly, the gate voltages where one of the CB's is lifted is where one of the wires goes through a resonance.

Note that although the effective action looks similar to the effective action for tunnel coupled quantum dots,<sup>22</sup> there is an important difference. Unlike the tunnel-coupled case [Fig. 7(a)], here, we have a two channel problem [Fig. 7(b)]. Hence, there is nonzero conductance even when only one of the Coulomb blockades is lifted. For instance, when the two dots are weakly capacitively coupled,  $(\mathcal{U}_1 - \mathcal{U}_2)$  is small), we can trivially see that when the CB through dot 1 is lifted,  $G_1 \neq 0$  and when the CB through dot 2 is lifted,  $G_2 \neq 0$ . Thus, if we measure the total conductance through both the dots, the lines of semimaxima are when one of the CBs is

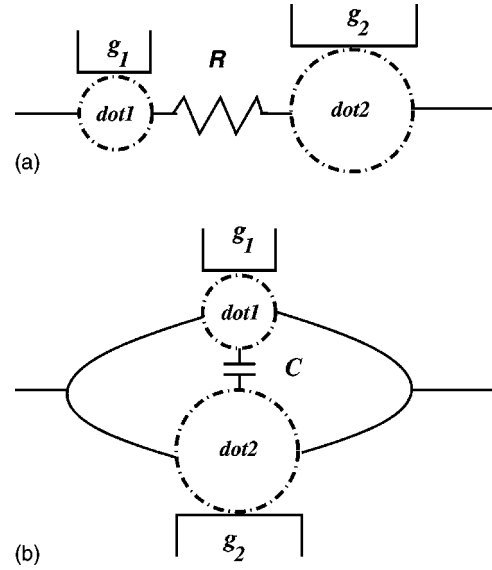


FIG. 7. Schematic diagram of (a) tunnel coupled quantum dots in series and (b) capacitively coupled quantum dots in parallel.

lifted and the points of maxima are when both CBs are lifted. In contrast, for the tunnel coupled dots, the maxima occur only when both Coulomb blockades are lifted.

When  $\mathcal{U}_1 \neq \mathcal{U}_2$ , we have a term mixing  $N_1$  and  $N_2$ . This tells us that the CB through one dot is affected by the charge on the other dot. As in the case of wires, this means that the CBs through both dots cannot be simultaneously lifted. The lines where one of the CBs is lifted is shifted from the  $\mathcal{U}_1 = \mathcal{U}_2$  case and as for the wires, we are unable to predict conductances at the crossing points. In contrast, the effect of a weak interdot coupling in the tunnel coupled case is to split the maxima.<sup>23,22</sup> These results are depicted in Fig. 8, to show the contrast.

#### V. DISCUSSIONS AND CONCLUSIONS

In this paper, we have studied conductance through a pair of carbon nanotubes, which are coupled by floating gates at the beginning and end of the wires. This geometry of carbon nanotubes enables us to study how resonant tunneling conductance through one carbon nanotube is affected by that of the other. We have obtained the conductance pattern as a function of the two gate voltages controlling the densities of the electrons in the two wires. In the plane of the two gate voltages, we find that (for identical carbon nanotubes), the conductance is a semimaximum (goes through a single resonance) along the lines  $g_2 - g_1 = -(m + 1/2)\mathcal{U}$  and  $g_1 + g_2 = (2k_F d / \pi) - (n + 1/2)\mathcal{U}$ . At the points where the two lines cross, the conductance is a maximum (goes through two resonances). In the rest of the plane, the conductance is very low (no resonance). When the two wires are not identical, the lines of semimaximum (single resonance) shift to  $g_1 - g_2 = [(2k_F d / \pi)((\mathcal{U}_1 - \mathcal{U}_2) / (\mathcal{U}_1 + \mathcal{U}_2)) - (n + 1/2) - (\pi / 4)((\mathcal{U}_1 - \mathcal{U}_2) / (\mathcal{U}_1 + \mathcal{U}_2))] 2\mathcal{U}_{\text{eff}}$  and  $g_1 + g_2 = [(2k_F d / \pi) - (m + 1/2) - (\pi / 4)((\mathcal{U}_1 - \mathcal{U}_2) / (\mathcal{U}_1 + \mathcal{U}_2))] 2\mathcal{U}_{\text{eff}}$  and there is no resonance when the lines cross. We have also mapped the

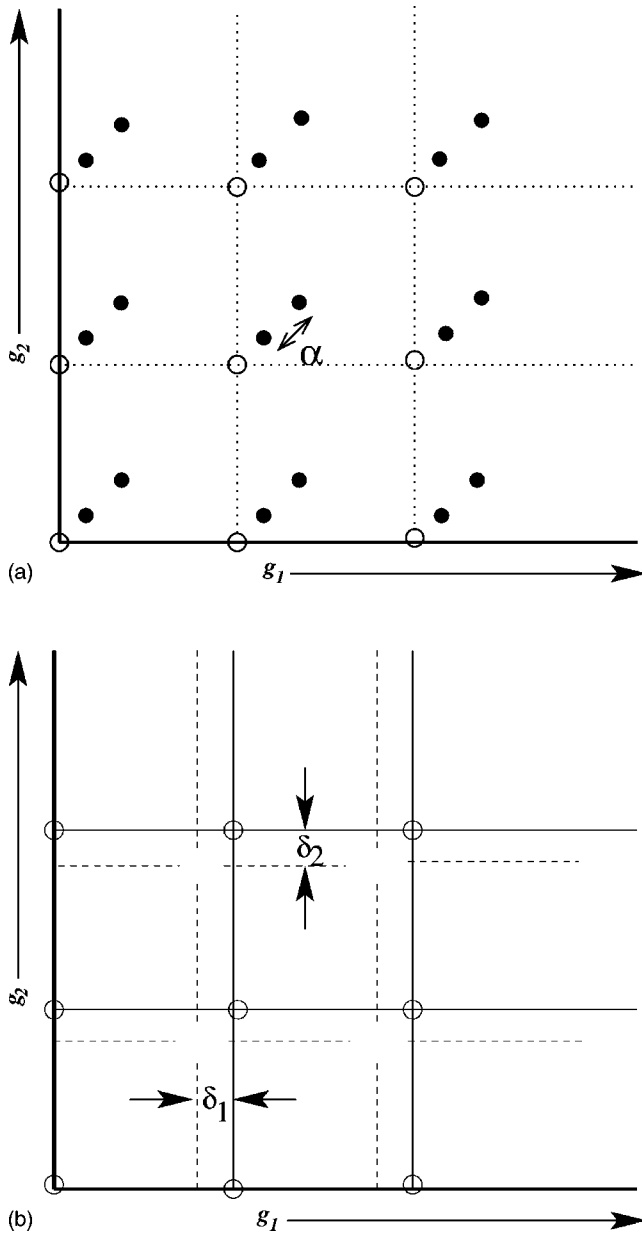


FIG. 8. Conductances in the plane of the gate voltages  $g_1$  and  $g_2$  for (a) tunnel coupled dots and (b) capacitively coupled dots. In the absence of coupling between the dots, the resonance maxima form a square grid in both cases as shown by the open circles. In (a), the open circles are the only points where there is a maxima, because both dots need to be at resonance. In (b), the solid lines indicate semimaxima (where one of the dots is on resonance) and the open circles denote maxima where both dots are at resonance. When interdot coupling is introduced, in (a), each point of resonance splits into two as shown by the solid circles. In (b), the lines of semimaxima shift as shown by the dotted lines, and there are no points where both dots are at resonance.

problem to that of two quantum dots that are capacitively coupled. The conductance through the double-dot system shows the same patterns of maxima when both the dots are on resonance, a semimaxima when one is on resonance and no conductance otherwise.

The above analysis has been a low temperature analysis,  $T \ll T_d = \hbar v_{\text{eff}} / K_{\text{eff}} d \sim 10$  K for typical wires of length  $d = 5 \mu\text{m}$ . This is needed for coherent propagation through the wire leading to resonance features. Hence, it is the length  $d$  which plays the role of a cutoff in the RG flows. Although, it may not be experimentally feasible to change the lengths of the wire, if it could be done, then one would expect the deviations of conductances from perfect resonance to scale as power laws of the lengths, as usually happens in LLs. The inclusion of leads also brings in nontrivial temperature dependences even in the low temperature limit. These may be experimentally easier to see. Thus such experiments would probe Luttinger liquid physics. More importantly, the geometry that we have studied also allows for cross-conductances, whose temperature and length dependencies also show the characteristic LL power laws. Here, however, the very existence of a “cross” current is an interaction dependent effect and thus provides a qualitative probe of LL physics. We should point out that single-walled carbon nanotubes with  $K_{\text{SWNT}} \sim 0.5-0.6$  are not in the strong coupling, strong interaction regime, which requires  $K < 0.5$  without leads, and  $K < 1/3$  with leads. However, it is quite likely that materials will be found which will be in the strong interaction regime. In this paper, we have given results both for weak and strong interaction strengths.

Qualitative tests of the other features that we have studied should also be experimentally feasible. Conductances through a double wire system or a capacitively coupled double dot system, should show the features that are seen in Figs. 4 and 8. There should be large differences in the conductance in the three different cases where (1) both the gate voltages are tuned to resonance (maxima of conductance), (2) when one of them is tuned to resonance (semimaxima of conductance), and (3) when both are out of resonance (very low conductance).

Finally, this analysis can be easily extended to the case where the two wires are allowed to ‘cross’ at more than two points. A very similar analysis shows that the system can still be decoupled in terms of “+” and “-” wires, in terms of which the problem reduces to that of Luttinger wires with multiple barriers.<sup>22</sup> For three crossings, the equivalent dot geometry involves four dots, at the four corners of a square, with tunnel couplings along the horizontal axis and capacitive couplings along the vertical axis. These are also interesting geometries to study<sup>24</sup> in the context of quantum computers.



- <sup>1</sup>S. J. Tans *et al.*, Nature (London) **386**, 474 (1997); M. Bockrath, D. H. Cobden, J. Lu, A. G. Rinzler, R. E. Smalley, L. Balents, and P. L. McEuen, *ibid.* **397**, 598 (1999).
- <sup>2</sup>Z. Yao, H. W. Postma, L. Balents, and C. Dekker, Nature (London) **402**, 273 (1999).
- <sup>3</sup>D. J. Bae, K. S. Kim, Y. S. Park, E. K. Suh, K. H. An, J. M. Moon, S. C. Lim, S. Y. Park, Y. H. Jeong, and Y. H. Lee, Phys. Rev. B **64**, 233401 (2001).
- <sup>4</sup>C. Kane, L. Balents, and M. P. A. Fisher, Phys. Rev. Lett. **79**, 5086 (1997).
- <sup>5</sup>B. Trauzettel, R. Egger, and H. Grabert, Phys. Rev. Lett. **88**, 116401 (2002).
- <sup>6</sup>C. Bena, S. Vishveshwara, L. Balents, and M. P. A. Fisher, Phys. Rev. Lett. **89**, 037901 (2002); C. S. Peca, L. Balents, and K. Wiese, Phys. Rev. B **68**, 205423 (2003).
- <sup>7</sup>A. Komnik and R. Egger, Phys. Rev. Lett. **80**, 2881 (1998).
- <sup>8</sup>J. Kim, K. Kang, J. Lee, H. Yoo, J. Kim, J. W. Park, H. M. So, and J. Kim, J. Phys. Soc. Jpn. **70**, 1464 (2001).
- <sup>9</sup>A. Komnik and R. Egger, Eur. Phys. J. B **19**, 271 (2000).
- <sup>10</sup>P. Durganandini and S. Rao, Phys. Rev. B **59**, 13 122 (1999).
- <sup>11</sup>P. Samuelson, E. Sukhorukov, and M. Buttiker, Doga: Turk. J. Phys. **27** 481 (2003).
- <sup>12</sup>R. Egger and A. O. Gogolin, Phys. Rev. Lett. **79**, 5082 (1997); Eur. Phys. J. B **3**, 281 (1998).
- <sup>13</sup>A. O. Gogolin and A. Komnik, Phys. Rev. Lett. **87**, 256806 (2001).
- <sup>14</sup>C. L. Kane and M. P. A. Fisher, Phys. Rev. B **46**, 15 233 (1992).
- <sup>15</sup>A. Furusaki and N. Nagaosa, Phys. Rev. B **47**, 4631 (1993).
- <sup>16</sup>M. Sassetti, F. Napoli, and U. Weiss, Phys. Rev. B **52**, 11 213 (1995).
- <sup>17</sup>M. Thorwart, M. Grifoni, G. Cuniberti, H. W. Ch. Postma, and C. Dekker, Phys. Rev. Lett. **89**, 196402 (2002).
- <sup>18</sup>S. Huegle and R. Egger, Europhys. Lett. **66**, 565 (2004).
- <sup>19</sup>I. Safi and H. J. Schulz, Phys. Rev. B **52**, 17 040 (1995); I. Safi, Ph.D. thesis, Laboratoire de Physique des Solides, Orsay, 1996.
- <sup>20</sup>S. Lal, S. Rao, and D. Sen, Phys. Rev. Lett. **87**, 026801 (2001); Phys. Rev. B **65**, 195304 (2002).
- <sup>21</sup>D. Goldhaber-Gordon, H. Shtrickman, D. Mahalu, D. Abusch-Magder, U. Meirav, and M. A. Kastner, Nature (London) **391**, 156 (1998).
- <sup>22</sup>S. Das and S. Rao, Phys. Rev. B **68**, 073301 (2003).
- <sup>23</sup>F. R. Waugh, M. J. Berry, D. J. Mar, R. M. Westervelt, K. L. Campman, and A. C. Gossard, Phys. Rev. Lett. **75**, 705 (1995); F. R. Waugh, M. J. Berry, C. H. Crouch, C. Livermore, D. J. Mar, R. M. Westervelt, K. L. Campman, and A. C. Gossard Phys. Rev. B **53**, 1413 (1996).
- <sup>24</sup>S. Das and S. Rao (unpublished).